

Polarization Properties of AGN at High Frequencies

S. G. Jorstad

*Institute for Astrophysical Research, Boston University, 725
Commonwealth Ave., Boston, MA 02215, USA*

Abstract. I discuss variability of polarization in the core region of parsec scale radio jets and connections between 7 mm polarization in the VLBI core and polarization at shorter wavelengths from the whole source for a sample of AGN with highly relativistic jets known as blazars. The sources show pronounced diversity in polarization behavior that is not clearly understood. I discuss possible reasons for these differences as well as the role that VSOP-2 can play in exploring the magnetic field in the most compact regions of jets.

1. Introduction

The current picture for jet formation in objects powered by accretion onto the black hole (BH) involves magnetic forces to produce, accelerate, and collimate the jet (see, e.g., Meier these proceedings). Investigations of structure of the magnetic field in jets of active galactic nuclei (AGN) should advance our understanding of this remarkable phenomenon and allow us to unveil processes that occur close to the central engine and are currently inaccessible to direct observation. The most straight way for studying the magnetic field is through linear polarization of the synchrotron emission emitted by AGN from radio to optical wavelengths. Such data, combined with imaging of the innermost part of the jet, have already produced fascinating results about the location of the polarized emission at different wavelengths within the jet and the connection between the magnetic field and jet direction (Wills et al. 1992; Lister & Smith 2000; Gabuzda et al. 2006; D’Arcangelo et al. 2007).

We have carried out a 3-yr monitoring program of 15 radio-loud, highly variable AGN that includes bimonthly total and polarized intensity imaging with the Very Long Baseline Array (VLBA) at 7 mm (43 GHz) along with simultaneous (within 1-2 week) polarization measurements at 3 mm (86 GHz), at 1 mm (230/350 GHz), and at optical wavelengths ($\lambda_{\text{eff}} \sim 640 \text{ nm}$). I will present the results of the program, which have been recently published (Jorstad et al. 2007) and will highlight the problems in our understanding of the jet structure that should be solved with the unprecedented resolution provided by the VSOP-2 mission.

2. A Polarization-Based Classification Scheme

Despite the small number of sources in our sample, we have found significant differences in their polarization properties that allow us to separate the sources

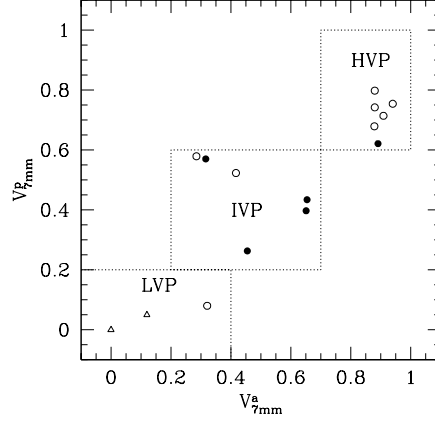


Figure 1. Connection between polarization and position angle variability indices in the VLBI core at 7 mm. Symbols denote the quasars (open circles), BL Lac objects (filled circles), and radio galaxies (triangles).

into three groups according to their polarization variability in the VLBI core at 43 GHz. We have characterized each source by two polarization variability indices, V_{7mm}^p and V_{7mm}^a :

$$V_{7mm}^p = \frac{(m_{7mm}^{\max} - \sigma_{m_{7mm}^{\max}}) - (m_{7mm}^{\min} + \sigma_{m_{7mm}^{\min}})}{(m_{7mm}^{\max} - \sigma_{m_{7mm}^{\max}}) + (m_{7mm}^{\min} + \sigma_{m_{7mm}^{\min}})}, \quad (1)$$

where m_{7mm}^{\max} and m_{7mm}^{\min} are, respectively, the maximum and minimum fractional polarization measured over all epochs in the VLBI core, and $\sigma_{m_{7mm}^{\max}}$ and $\sigma_{m_{7mm}^{\min}}$ are the corresponding uncertainties.

$$V_{7mm}^a = \frac{|\Delta\chi_{7mm}| - \sqrt{\sigma_{\chi_{7mm}^1}^2 + \sigma_{\chi_{7mm}^2}^2}}{90}, \quad (2)$$

where χ_{7mm} is electric vector position angle in the VLBI core measured at 7 mm, $\Delta\chi_{7mm}$ is the observed range of polarization direction and $\sigma_{\chi_{7mm}^1}$, $\sigma_{\chi_{7mm}^2}$ are the uncertainties in the two values of EVPAs that define the range. We treat the 180° ambiguities in EVPAs such that $\Delta\chi_{7mm}$ does not exceed 90° . In both cases, if $V^a \leq 0$ ($V^p \leq 0$) then we set $V^a = 0$ ($V^p = 0$) and conclude that the observations were unable to measure variability in the polarization position angle.

We have based our classification on a strong correlation between variability indices V^p and V^a (Fig. 1, coefficient of correlation $r=0.83$) that produces a separation of the sources into three groups: **LVP** – low variability of polarization in the radio core, $V_{7mm}^p \leq 0.2$, $V_{7mm}^a \leq 0.4$; **IVP** – intermediate variability of polarization, $0.2 < V_{7mm}^p \leq 0.6$, $0.2 < V_{7mm}^a \leq 0.7$; and **HVP** – high variability of polarization in the radio core, $V_{7mm}^p > 0.6$, $V_{7mm}^a > 0.7$. The LVP group includes the two radio galaxies 3C 111 and 3C 120 plus the low optically polarized quasar 3C 273. The IVP group consists of four (out of five) BL Lac objects and two

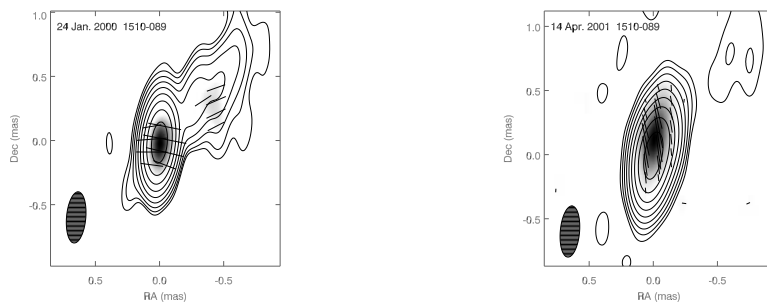


Figure 2. 43 GHz total and polarized intensity images of the quasar 1510-089 obtained at two different epochs, which reveal significantly different EVPAs (solid sticks) in the core of the quasar; the absolute calibration of the EVPAs is the result of consistency between different methods (see Jorstad et al. 2007).

highly optically polarized quasars, 3C 279 and 3C 345. The majority of the quasars (five out of eight) and one BL Lac object, OJ 287, form the HVP group. Figure 2 shows a change in the EVPA of about 90° in the core of the quasar 1510-089, which belongs to the HVP group. This classification roughly - but with some exceptions - follows the classical separation of AGN into radio galaxies (LVP), BL Lac objects (IVP), and quasars (HVP). Our analysis of the jet kinematics (Jorstad et al. 2005) reveals that the radio galaxies have the smallest Lorentz factor ($\Gamma \sim 5$) and the largest viewing and opening angles ($\Theta_o \sim 20^\circ$ and $\theta_o \sim 3^\circ$, respectively) while the HVP quasars have the highest Lorentz factor, $\Gamma > 20$, and the smallest viewing and opening angles ($\Theta_o \sim 2^\circ$ and $\theta_o \sim 0.5^\circ$).

3. Faraday Rotation in the Inner Jet

In the IVP and HVP sources the EVPAs in the VLBI core at 7 mm and at shorter mm-wavelengths from the whole source (simultaneous within 1-2 days) show some rotation of the polarization position angle with wavelength. Assuming that the contribution in the polarized flux from the emission outside the core is negligible at 1-3 mm (this is most likely true when there is no new knot emerging from the core), we have attributed this rotation to Faraday rotation by a foreground screen close to the VLBI core (Zavala & Taylor 2004). We have defined the rotation measure RM by assuming that at 1 mm we see the unrotated direction of the polarization and that the emission from 1 mm to 7 mm propagates through the same screen (see some examples in Fig. 3). Derived values of rotation measure tentatively show that the HVP sources have higher rotation measures, $\langle |RM^\circ| \rangle = (8.5 \pm 6.5) \times 10^4 \text{ rad m}^{-2}$, than the IVP sources, $\langle |RM^\circ| \rangle = (1.1 \pm 0.3) \times 10^4 \text{ rad m}^{-2}$, where RM° is the intrinsic rotation measure, $RM^\circ = RM (1+z)^2$. Even larger rotation measure can be expected for the LVP sources, since in the LVP sources the core at 7 mm is unpolarized. We have computed the polarization parameters of the inner jet by summing the polarization of VLBI components within a few mas of the core. Highly polarized

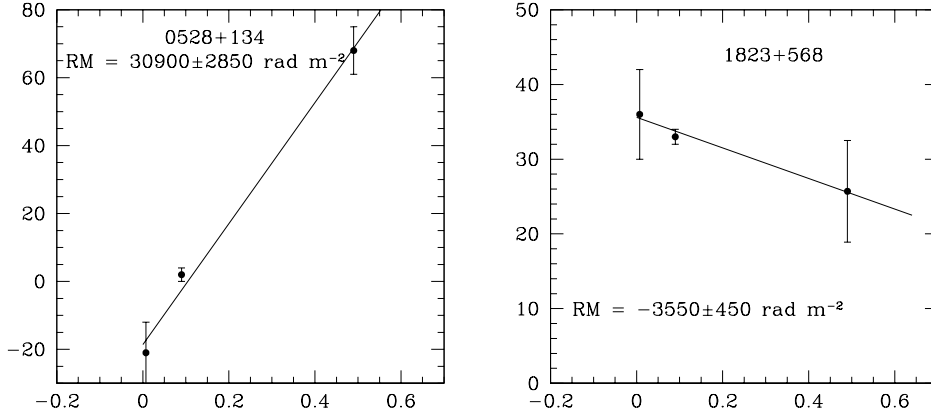


Figure 3. Dependence of polarization position angle on square of wavelength in the quasar 0528+134 (HVP) and BL Lac object 1823+568 (IVP). The solid line represents an approximate fit to the dependence by a λ^2 Faraday rotation law.

components are usually present in jets of the LVP sources (Jorstad et al. 2007). Figure 4 (*left*) shows that there is good correspondence between the degree of polarization in the quasar 3C 273 at 1 mm from the whole source and at 7 mm from the inner jet. Similar behavior is observed for 3C 111 and 3C 120. This implies that in the LVP sources the 1 mm and 3 mm cores have low polarization as well, so that the polarization comes completely from the knots. Attridge et al. (2005) have found a very high rotation measure near the core of 3C 273, $RM = 2.1 \times 10^4 \text{ rad m}^{-2}$. The low polarization of the core could be the result of either fine-scale turbulence or depolarization by a very thick, inhomogeneous foreground screen with $RM > 5 \times 10^5 \text{ rad m}^{-2}$, as suggested by Attridge et al. (2005).

For some sources in our sample the rotation measure in the VLBI core has been determined using lower frequencies (Zavala & Taylor 2004; Gabuzda et al. 2006). Figure 4 (*right*) compares rotation measures obtained from different sets of frequencies, revealing an increase of the rotation measure with frequency. This can be interpreted as the result of a decrease of the rotation measure with distance from the central engine, since the location of the core from the central engine depends on the frequency of the observation owing to optical depth effects. The decrease in RM reflects a decrease in thickness of the Faraday screen and/or in strength of the magnetic field component parallel to the line of sight with distance from the BH (see also O’Sullivan, these proceedings). For the IVP and HVP sources we have corrected EVPAs at 3 mm and 7 mm for the Faraday rotation measure.

4. Comparison of Polarization at Different Wavelengths

Comparison between the degree of polarization at optical, 1 mm, and 3 mm wavelengths from the whole source with respect to the degree of polarization

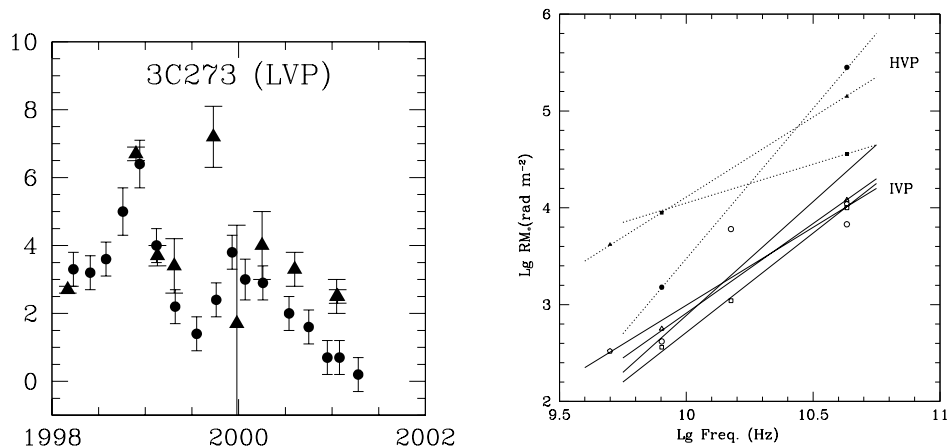


Figure 4. *Left:* Degree of polarization in the inner jet at 7 mm (circles) and at 1 mm from the whole source (triangles) in the quasar 3C 273. *Right:* Dependence of rotation measure on frequency in the IVP (open symbols and solid lines) and HVP sources (filled symbols and dashed lines). The rotation measure is referred to the lowest frequency among the frequencies used to determine the rotation measure.

measured in the VLBI core at 7 mm for the closest observations obtained at opt-7 mm, 1-7 mm, and 3-7 mm wavelengths for each source (these measurements are simultaneous within 1-3 days) indicates a statistically significant correlation. However, the optical polarization maintains the strongest connection to the polarization in the VLBI core ($r=0.87$). The dependence between bulk Lorentz factor (Jorstad et al. 2005) and polarization variability index, V^P , indicates that the strongest connection is observed between Γ and $V_{7\text{mm}}^P$ ($r=0.72$) and between Γ and V_{opt}^P ($r=0.53$), while the polarization variability index at 1 mm does not correlate with the Lorentz factor ($r=-0.12$). For the IVP and HVP sources we have computed values of deviation between optical and mm-wave EVPAs for measurements obtained within 2 weeks of each other (EVPAs at 7 mm correspond to the EVPAs in the VLBI core). In the IVP sources an excellent agreement exists between polarization position angle at different wavelengths. For the HVP sources, the result is qualitatively different, with the best agreement observed between optical EVPA and polarization position angle in the core at 7 mm, while the polarization position angle at 1 mm does not show any connection with the optical polarization position angle. The fact that the optical polarization does show the correlation with the polarization in the core at 7 mm, as well as the best alignment of position angle with the electric vector in the core at 7 mm, implies that most of the nonthermal optical emission arises close to the 7 mm core, most likely in shocks, while another emission component in addition to transverse shocks is prominent at 1 mm. A primary candidate for this component is the “true” core, i.e., the bright, narrow end of the jet when observed at a wavelength where the emission is completely optically thin (Marscher 1995). The true core does not possess relativistic electrons energetic enough to produce the optical synchrotron emission; shocks are needed to do so.

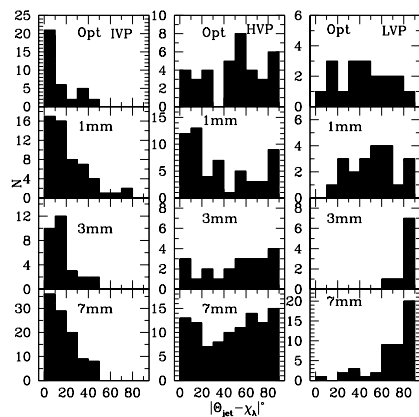


Figure 5. Distributions of offsets between polarization position angle and jet direction.

We have compared the polarization position angle, χ_λ , for each polarization measurement with the position angle of the jet projected on the sky, Θ_{jet} . Θ_{jet} corresponds to the VLBA epoch nearest to a given polarization measurement. The distributions of the offsets between direction of polarization and jet axis are presented in Figure 5. Figure 5 shows that the properties of polarization position angle with respect to the jet direction are distinct for each group and similar at different frequencies within a group: good alignment of the electric vector with the jet direction in the IVP sources, chaotic behavior of the electric vector in the HVP blazars, and electric vector preferentially transverse to the jet direction in the LVP objects at 3 mm and in the inner jet at 7 mm. These differences between the groups can be caused by differences (i) in intrinsic magnetic field structure; (ii) in shock strength; (iii) in thickness of the Faraday screen near the core; and (iv) in kinematic and structure of the jets. To understand what is responsible for the observed diversity as well as to explore properties of the true core, we need the unique resolution of VSOP-2 combined with the highest resolution possible for ground-based VLBI observations.

Acknowledgments. This material is based on work supported by the National Science Foundation under grant no. AST-0406865. The author is thankful to the organization and science committee for the fruitful meeting and wishes Prof. Harabayashi great achievements in inspiring a new generation of scientists.

References

- Attridge, J. M. et al. 2005, ApJ, 633, L85
D’Arcangelo, F. D. et al. 2007, ApJ, 659, L107
Gabuzda, D. C. et al. 2006, MNRAS, 369, 1596
Jorstad, S. G. et al. 2007, AJ, 134, 799
Jorstad, S. G. et al. 2005, AJ, 130, 1418
Lister, M. L., & Smith, P. S. 2000, ApJ, 541, 66
Marscher, A. P. 1995, Proc. of the National Academy of Sciences, 92, 11439
Wills, B. J. et al. ApJ, 398, 454
Zavala, R. T., & Taylor, G. B. 2004, ApJ, 612, 749